Great Britain Journals Press

RESEARCH FINGERPRINT

IDENTIFIER
LJRS-226228

PEER REVIEW
Double Blind

SIMILARITY CHECK
Perplexity AI and iThenticate

ACCESS
Open Access

LANGUAGE
English

PRINT ISSN
2631-8490

ONLINE ISSN
2631-8504

EDITION

ABBREVIATION
LJRS

VOLUME
26

ISSUE
5

YEAR
2026

KEY DATES

RECEIVED
2026-03-06

ACCEPTED
2026-03-12

CATALOGING

CROSSMARK DOI
10.34257/LJRS226228UK

PACS CLASS
42.65.Dr, 42.65.Ky

INSPEC CLASS
A4265C

ARXIV CLASS
physics.optics

ACCESS ONLINE

Article Record

Quasi-Phase Matching Generation of the Anti-Stokes Component at Stimulated Raman Scattering

CORRESPONDENCE

AUTHORS & AFFILIATIONS

Dr. Rena J. Kasumova ¶*

¶ Physics Department, Baku State University, Baku, Az (OA)

ABSTRACT

We propose an analytical method for calculating the parameters of quasi-phase matching generation of the anti-Stokes component at stimulated Raman scattering in layered media. We present the results of the analysis in CIA considering losses and changes in the phases of all interacting waves. We consider frequency conversion processes in a layered structure consisting of periods of a “lattice” of modulation of the nonlinear susceptibility. Moreover, the values of the complex amplitudes of the pump radiation and the scattering components at the output of each layer are the input values of the corresponding complex amplitudes for the next layer. We give analytical expressions for the intensity of the transformation into the anti-Stokes component. We analyze the factors that limit the efficiency of the frequency conversion process. We calculated the maximum conversion efficiency to the anti-Stokes component in compressed hydrogen for a three-layer structure.

Index Terms: stimulated Raman scattering • anti-Stokes generation • quasi-phase matching • hydrogen • constant intensity approximation

FUNDING
No external funding was declared for this work.

CONFLICTS
The authors declare no conflict of interest.

AI USAGE
No generative AI was used for analysis or results.

HOW TO CITE
Kasumova (2026). Quasi-Phase Matching Generation of the Anti-Stokes Component at Stimulated Raman Scattering. London Journal of Research In Science: Natural and Formal, 26(5), 15-20. DOI: 10.34257/LJRS226228UK

METADATA CONTINUATION

AUTHOR CONTACT QR LEDGER

Dr. Rena J. Kasumova¶*

ARCHIVAL RECORD

LJRS · Vol 26 · Issue 5 · 2026

Article ID LJRS-226228 · DOI 10.34257/LJRS226228UK

Print ISSN 2631-8490 · Online ISSN 2631-8504

CROSSREF DOI 10.34257/LJRS226228UK

RESEARCH ARTICLE

Quasi-Phase Matching Generation of the Anti-Stokes Component at Stimulated Raman Scattering

Dr. Rena J. Kasumova[¶*]

AFFILIATIONS

¶ Physics Department, Baku State University, Baku, Az (**OA**)

Abstract

We propose an analytical method for calculating the parameters of quasi-phase matching generation of the anti-Stokes component at stimulated Raman scattering in layered media. We present the results of the analysis in CIA considering losses and changes in the phases of all interacting waves. We consider frequency conversion processes in a layered structure consisting of periods of a "lattice" of modulation of the nonlinear susceptibility. Moreover, the values of the complex amplitudes of the pump radiation and the scattering components at the output of each layer are the input values of the corresponding complex amplitudes for the next layer. We give analytical expressions for the intensity of the transformation into the anti-Stokes component. We analyze the factors that limit the efficiency of the frequency conversion process. We calculated the maximum conversion efficiency to the anti-Stokes component in compressed hydrogen for a three-layer structure.

Keywords: *stimulated Raman scattering, anti-Stokes generation, quasi-phase matching, hydrogen, constant intensity approximation*

Correspondence: Dr. Rena J. Kasumova

1 Introduction

Researchers use the anti-Stokes component generated by stimulated Raman scattering (SRS) when probing the atmosphere, the aquatic environment, to control the process of oil drilling, spectroscopy of molecules. Spectroscopy of anti-Stokes light scattering is a powerful tool for studying fast molecular processes in gases and liquids. This also includes the SRS technique, active Raman spectroscopy, non-stationary processes at stimulated scattering. In these applications, to increase the sensitivity of probing, it is necessary to increase the signal level of the anti-Stokes component of Raman scattering, which carries information about temperature changes in the probing space.

Research on increasing the conversion efficiency of the anti-Stokes scattering component will not lose its relevance for a long time. It is enough just to note one area of application - the use of Raman scattering for the development of temperature sensors. Modern standard distributed temperature sensor (DTS) systems record well-temperature changes. This enables timely reaction to oil-well drilling and optimization of its operation. The intensity of the Raman scattering anti-Stokes component that carries information about temperature changes in the monitored space must be increased for more effective temperature monitoring of the process.

According to experimental studies, the qsignal level of the anti-Stokes component can be increased by $3-6\%$ due to focusing [1-2], also due to operation in the phase-matching mode by 15% [3]. It is known that the inverted domain layers can be used to increase the frequency conversion intensity [4-5]. The quasi-phase matching interactions that arise in this case lead to phase correction, as a result, to a high efficiency of frequency conversion compared to conversion in a conventional volume medium. This is in demand when it is practically difficult to implement the fulfillment of the phase matching condition. For example, in compressed hydrogen at a pressure of 30 atm, the implementation of phase matching is accompanied by technical difficulties: it is necessary to implement the propagation of collimated beams with an angular divergence $\leq 1^o$ with an accuracy of 1 μrad at distances of about 1 m [3]. Currently, quasi-phase-matched interactions in periodically polarized inverted crystals with counterpropagating waves are being intensively studied [6-8].

In [9-10], for increasing the efficiency of the signal of the anti-Stokes component of SRS, the authors propose to vary the nonlinear cubic susceptibility in layered media. In this case, the layers contain Raman active nonlinear media and passive media without nonlinearity. In [11], it was experimentally obtained that such a passive layer can be obtained using such a nonlinear effect as the optical Stark effect. The authors of [11] experimentally found that by applying such a nonlinear effect as the optical Stark effect, one could obtain a similar passive layer. The shift of levels in the field of a light wave leads to a shift in the spectral scattering lines. Excitation by laser fields leads to a significant shift of the scattering component. Obtaining such a displacement in a constant electric field requires high intensities of the order of breakdown values and higher. Hence, the action of the electric field of laser radiation with a strength sufficient for the spectral shift leads to the absence of amplification of Stokes radiation in this layer. The so-called passive layers are implemented using this fact. In [9-10], the authors use a numerical method for studying the quasiphase matching interaction in such a layered Raman-active medium using the first-order Euler method. In the works [12-16] authors theoretically studied quasi- phase matching interactions in periodic nonlinear structures.

The authors analyze the frequency transformations in the constant field approximation (CFA) or by numerical methods. In CFA, the amplitude and phase of the pump radiation are constant, and the coherent length of the nonlinear medium depends solely on the detuning of the wave vectors. However, this simplification is valid only at the beginning of the interaction, when the effect of the excited wave on the pump wave is small and pump depletion ignored. As a result, we do not consider a few features of the nonlinear process. A direct numerical calculation of the coupled equations for each layer is possible. However, the use of the analytical method makes it possible to obtain the optimal parameters of the problem from specific analytical expressions and give recommendations for achieving maximum conversion efficiency. Therefore, it is expedient to use the constant intensity approximation (CIA), which considers the back reaction of the excited wave to the pump wave [17]. In this approximation, the coherent length, in addition to the detuning of the interacting waves, depends on such parameters of the problem as the intensities of the main radiation, Stokes (anti-Stokes) component and losses in the medium. In this approximation we considered second harmonic generation, sum frequency generation, third harmonic generation in regular domain structures (RDS), and intracavity conversion from which we will cite one of these works, for example [18]. In addition, we considered spontaneous Raman scattering of the Stokes and anti-Stokes components at intracavity transformation [19] and at CARS in optic fiber [20]. In this work, to calculate the parameters of quasi-phase-matched generation of the anti-Stokes component of SRS in a layered structure, we use this analytical method. Frequency conversion processes in a layered structure consisting of periods of a “lattice” of modulation of the nonlinear susceptibility are considered. Moreover, the values of the complex amplitudes of the pump radiation and the scattering components at the output of each layer are the input values of the corresponding complex amplitudes for the next layer. We obtained analytical expressions for the conversion efficiency to the anti-Stokes component and analyzed the factors that limit the efficiency of the frequency conversion process.

2 Theory

Let us consider the quasi-phase matching interaction of waves at the generation of the anti-Stokes SRS component in a medium with a periodic structure. The structure consists of a few successive layers with periodically changing values of the cubic susceptibility. We carry out the analytical analysis according to the procedure we used in [18].

To study these processes, it is necessary to solve truncated equations that describe the process of generation of the anti-Stokes SRS component in each of the layers separately. At all stages, the problem is solved with the appropriate boundary conditions, namely, the output parameters of the previous layer are the input parameters of the next layer. Let us consider SRS of the Stokes and anti-Stokes components under the action of a laser pump wave in the first layer with a Raman active medium with cubic susceptibility $\chi^{(3)}$. To describe these processes in the quasi-stationary case, the system of wave equations has the form [4, 21]:

$$\begin{aligned}
&\frac{dA_p}{dz} + \delta_p A_p = -i\big[\gamma_p^s |A_s|^2 A_p + \gamma_p^{sa} A_p^* A_s A_a e^{-i\Delta z} + \gamma_p^a |A_a|^2 A_p\big],\\
&\frac{dA_s}{dz} + \delta_s A_s = -i\left[\gamma_s |A_p|^2 A_s + \gamma_s^{sa} A_p^2 A_a^* e^{i\Delta z}\right],\\
&\frac{dA_a}{dz} + \delta_a A_a = -i\left[\gamma_a |A_p|^2 A_a + \gamma_a^{sa} A_p^2 A_s^* e^{i\Delta z}\right],
\end{aligned} \tag{1}$$

where

$$\begin{aligned}
&\gamma_p^s = \frac{2\pi\omega_p}{cn_p}\chi_s^{(3)*}(\omega_p = \omega_s - \omega_s + \omega_p),\\
&\gamma_p^{sa} = \frac{2\pi\omega_p}{cn_p}\left[\chi_{sa}^{(3)*}(\omega_p = \omega_a + \omega_s - \omega_p) + \chi_{sa}^{(3)*}\right],\\
&\gamma_p^a = \frac{2\pi\omega_p}{cn_p}\chi_a^{(3)}(\omega_p = \omega_a - \omega_a + \omega_p),\\
&\gamma_s = \frac{2\pi\omega_s}{cn_s}\chi_s^{(3)}(\omega_s = \omega_p - \omega_p + \omega_s),\\
&\gamma_s^{sa} = \frac{2\pi\omega_s}{cn_s}\chi_{sa}^{(3)}(\omega_s = 2\omega_p - \omega_a),\\
&\gamma_a = \frac{2\pi\omega_a}{cn_a}\chi_a^{(3)}(\omega_a = \omega_p - \omega_p + \omega_a),\\
&\gamma_a^{sa} = \frac{2\pi\omega_a}{cn_a}\chi_{sa}^{(3)*}(\omega_a = 2\omega_p - \omega_s).
\end{aligned}$$

Here, $A_{p,s,a}$ the complex amplitudes of the pump wave, the Stokes and anti-Stokes components at frequencies $\omega_{p,s,a}, \gamma_i\ (i = s, a), \gamma_p^{s,a}$ are the nonlinear coupling coefficients at SRS of the Stokes and anti-Stokes components, $\gamma_{p,s,a}^{sa}$ anti-Stokes components, $\delta_{p,s,a}$ and $n_{p,s,a}$ determine the linear losses and refractive indices at the corresponding frequencies $\omega_{p,s,a}$. $\Delta = 2k_p - k_s - k_a$ denotes the phase mismatch of the wave vectors, the waves propagate in the positive direction of the z axis.

In the general case, the cubic susceptibility contains resonant and nonresonant parts. However, for most purely Raman media [21-22], the actual nonresonant electronic susceptibility is small compared to the resonant part, so we do not take it into account in our calculations below. We carry out the consideration for the case of exact frequency resonance when the cubic susceptibility $\chi_{p,s,a}^{(3)}$ p .

We consider the generation of the anti-Stokes scattering component at SRS considering the losses of all interacting waves in the general case, when both the pump wave and the Stokes component wave are present at the input to the first layer of length l_1 . Then the boundary conditions at the input have the form:

$$A_{p,s}(z=0) = A_{po,so}\exp(i\varphi_{po,so}), \quad A_a(z=0)=0, \tag{2}$$

where $z = 0$ corresponds to the input to the first layer and $\varphi_{po,so}$ are the initial values of the phase of the pump wave and the Stokes component at the input to the first layer.

Solving system (1) in CIA, i.e. $I_p(z=0) = I_{po}$ $I_s(z=0) = I_{so}$, considering (2), for the complex amplitude of the anti-Stokes component at the output of the first layer, we obtain

$$A_a(z=l_1) = -i\gamma_a^{sa}A_{po}^2A_{so}^*\frac{\sin\lambda_1^a l_1}{\lambda_1^a}\cdot\exp\left[-\frac{\delta_a+\delta_s+2\delta_p+i(\gamma_1^a-\lambda)}{2}l_1+i(2\varphi_{po}-\varphi_{so})\right], \tag{3}$$

where

$$\gamma_1^a = 2\gamma_p^s I_{so} + \gamma_a I_{po} - \gamma_s^* I_{po}.I_j = A_j\cdot A_j^*,$$
$$\lambda_1^a = \sqrt{\gamma_a^{sa}I_{po}(2\gamma_p^{sa}I_{so}-\gamma_s^{sa}I_{po}) - \frac{\left[\delta_a\cdot\hat{\delta}_s-2\delta_p+i(\gamma_aI_{po}+\gamma_s^*I_{po}-2\gamma_p^SI_{so}+\hat{A})\right]^2}{4}}.$$

Under the conditions $(\gamma_a+\gamma_s^*)I_{po} = 2\gamma_p^sI_{so}$ and $\delta_s+2\delta_p=\delta_a$ we get $\lambda_1^a \doteq \sqrt{\frac{\Delta^2}{4}-\Gamma_a^2}, \Gamma_a^2 = \gamma_a^{sa}I_{po}(\gamma_s^{sa}I_{po}-2\gamma_p^{sa}I_{so})$ $l_{1,coh}^{CIA} = 0.5\pi/\sqrt{\frac{\Delta^2}{4}-\Gamma_a^2}$. And in the case of CFA ($\gamma_{p,s}^{sa}=0,\ \gamma_p^{s,a}=0,\ \gamma_s=0$) , a similar expression is $\lambda_1^{aCFA} = \Delta/2$ and $l_{1,coh}^{CFA} = \pi/\Delta$. Let us compare the expressions for coherent lengths in both approximations. In CIA, the coherent length and phase of the anti-Stokes wave depend, in addition to the phase mismatch Δ , on the intensities of the pump and Stokes waves.

Neglecting losses, from (3) we obtain

$$A_a(z=l_1) = -i\gamma_a^{sa}A_{po}^2A_{so}^*\frac{\sinh\lambda_1^{a\prime\prime}l_1}{\lambda_1^{a\prime\prime}}\cdot\exp\left[-i\frac{\gamma_1^a-\mathcal{A}}{2}l_1+i(2\varphi_{po}-\varphi_{so})\right], \tag{4}$$

where

$$\lambda_1^{a\prime\prime} = \sqrt{\frac{\left[(\gamma_aI_{po}+\gamma_s^*I_{po}-2\gamma_p^sI_{so}+\Delta)\right]^2}{4}+\Gamma_a^2}.$$

From (4) one can obtain an expression for the intensity $I_a(l_1)$.

Now we use the analysis applied above for the anti-Stokes component for the case of the Stokes scattering component. To do this, we will solve system (1) with respect to the complex amplitude of the Stokes component in CIA, i.e., at the input $I_p(z=0)=I_{po}, I_a(z=0)=I_{ao}=0$. Considering the boundary conditions (2), at the output of the first layer, we obtain $(\delta_{p,s,a}=0)$

$$A_s(z=l_1) = A_{so}\left[\cos\lambda_1^sl_1 - i\left(\gamma_sA_{po}^2\exp(i2\varphi_{po})-\frac{\gamma_1^s-\Delta}{2}\right)\frac{\sin\lambda_1^sl_1}{\lambda_1^s}\right]\cdot\exp\left(i\varphi_{so}-i\frac{\gamma_1^s-\Delta}{2}l_1\right) \tag{5}$$

$$\lambda_1^s = \sqrt{\gamma_s^{sa}\gamma_a^{sa}I_{po}^2 - \frac{(\gamma_sI_{po}+\gamma_a^*I_{po}-2\gamma_p^SI_{so}+\Delta)^2}{4}}, \gamma_1^s = 2\gamma_p^sI_{so}+\gamma_sI_{po}-\gamma_a^*I_{po}.$$

From (5) one can obtain an expression for the intensity $I_s(l_1)$. It follows from (5) that with increasing pump power, the maximum conversion to the Stokes component occurs at shorter coerent lengths. From (5) one can also find the optimal value of the pump intensity or obtaining the maximum signal of the Stokes component.

In further analytical expressions, we do not consider wave losses in order to avoid cumbersome formulas. Substituting (4) into the third equation of system (1), for the complex amplitude of the pump wave at the exit from the first layer, we obtain

$$\begin{aligned} A_p^2(l_1) = &\left\{\frac{A_{so}^*A_{po}^2}{A_s^*(l_1)}\left[\cos\lambda_1^al_1 - i\frac{(\gamma_1^a-\Delta)}{2}\frac{\sin\lambda_1^al_1}{\lambda_1^a}\right]\right.\\ &\left.\times\exp\left[i(2\varphi_{po}-\varphi_{so})-i\frac{\gamma_1^a-\Delta}{2}\right]+i\frac{\gamma_a}{\gamma_a^{sa}}\frac{A_a(l_1)}{A_s^*(l_1)}I_{po}\right\}\times\exp(-i\Delta l_1)\end{aligned} \tag{6}$$

Let us calculate the phases of the pump wave and the anti-Stokes component in the first layer. In system (1), we make a change: $A_j(z) = a_j(z)\cdot\exp(i\varphi_jz)$, $j=p,s,a$. Applying the standard procedure used in [23], we obtain the phase of the pump wave in CIA:

$$\varphi_p(z) = \varphi_{po} + \gamma_p^{sa}\gamma_a^{sa}I_{p0}I_{so}\left(\gamma_aI_{p0}+\frac{\Delta-\gamma_1^a}{2}\right)\frac{z}{2\lambda_1^{a^2}}[1-\mathrm{sinc}(2\lambda_1^az)] - \gamma_p^sI_{so}z, \tag{7}$$

For comparison, in the CFA $\varphi_p(z) = \text{const.}$, since in this approximation the phase of the pump wave is constant.

Similarly, for the anti-Stokes component, we obtain an expression for the phase:

$$\varphi_a(z) = (\Delta-\gamma_1^a)z/2 - \pi/2 + 2\varphi_{po} - \varphi_{so}. \tag{8}$$

Now consider the behavior of complex amplitudes $A_{p,s,a}$ in the second layer, which has no non-linearity (therefore, this layer is passive). In this case, the initial values of the complex wave amplitudes are determined by their values at the end of the first layer from expressions (3) and (4), i.e. boundary conditions have the form:

$$A_{p,s,a}(z=l_1) = A_{p,s,a}(l_1)\exp[i\varphi_{p,s,a}(l_1)]. \tag{9}$$

Here $\varphi_{p,s,a}(l_1)$ are the changes in the phase of the waves at the transition from the first layer to the second at frequencies $\omega_{p,s,a}$, respectively, $z = 0$ again corresponds to the input, but already $l_1 = l_{1,coh}^{CIA}$

Since the absorption of waves is not considered, when passing through the second layer (passive), in which $\chi_{s,a,sa}^{(3)} = 0$, we have at the output of the second layer of length l_2:

$$\begin{aligned} A_p(z = l_2) &= A_p(l_1)\exp[i\varphi_p(l_1) + i\varphi_p(l_2)], \\ A_s(z = l_2) &= A_s(l_1)\exp[i\varphi_s(l_1) + i\varphi_s(l_2)], \\ A_a(z = l_2) &= A_a(l_1)\exp[i\varphi_a(l_1) + i\varphi_a(l_2)]. \end{aligned} \tag{10}$$

It should be noted that in RDS with quadratic and cubic nonlinearity, the quasi-phase matching condition (i.e., compensation of the phase mismatch between interacting waves) was satisfied by changing the sign of the nonlinear polarization for neighboring layers-domains. Analytically, this was considered by changing the sign of the nonlinear coefficients when passing from layer to layer, which is equivalent to changing the generalized phase by an amount equal to π .

In the case under study, the phase mismatch of waves equal to π , which occurs in a Ramanactive medium, is compensated in the second passive layer. Compensation is due to the optical Stark effect. It also provides a change in the generalized phase waves in the passive layer (ψ_2) by π [9], i.e., one can write:

$$\psi_2 = 2\varphi_p(l_2) - \varphi_a(l_2) - \varphi_s(l_2) = \pi.$$

Thus, the quasi-phase-matching condition is satisfied in the passive layer. Therefore, all three waves will enter the third layer without phase mismatch. Hence, in this layer, the intensity of the anti-Stokes component further increases up to the coherent length of the third layer. In terms of energy, this leads to further energy transfer from the pump wave and the Stokes component to the anti-Stokes component.

Consider the behavior of complex amplitudes $A_{p,s,a}$ in the third layer, which is nonlinear. In this case, the initial values of the complex wave amplitudes at the input to the third layer are equal to their output values at the end of the second layer, i.e. conditions (8)–(10). The boundary conditions have the form:

$$A_p(z = 0) = A_p(l_2), \quad A_s(z = 0) = A_s(l_2), \quad A_a(z = 0) = A_a(l_2). \tag{11}$$

Here $z = 0$ again corresponds to the entrance, but already in the third layer.

The behavior of complex amplitudes in this case is also described by system (1), however, the corresponding nonlinear coupling coefficients and the phase mismatch of the waves in the third layer will be denoted by dashes. In CIA, solving system (1) considering the boundary conditions (11), for the complex amplitude of the anti-Stokes component at the output of the third layer, $z = l_3$, we obtain:

$$\begin{aligned} A_a(l_3) = A_a(l_2)\left\{\cos\lambda_3^a l_3 + \left[\frac{\gamma_a^{sa\prime}}{\gamma_a^{sa}}\left(\lambda_1^a ctg(\lambda_1^a l_1) + \gamma_a I_{po} + i\frac{\Delta - \gamma_1^a}{2}\right)e^{i\psi} - i\left(\gamma_3 + \frac{\Delta'}{2}\right)\right]\frac{\sin\lambda_3^a l_3}{\lambda_3^a}\right\} \\ \times\exp\left[i\varphi_a(l_2) - i\frac{\gamma_3^a - \Delta'}{2}l_3\right], \end{aligned} \tag{12}$$

where

$$\begin{aligned} \gamma_3 &= \tfrac{\gamma_{a'} + \gamma_s^{*\prime}}{2} I_p(l_1) - \gamma_p^s / I_s(l_1), \\ \lambda_3^a &= \sqrt{\gamma_a^{sa} I_p(l_1)[2\gamma_p^{sa} I_s(l_1) - \gamma_s^{sa} I_p(l_1)] + \tfrac{(\gamma_a I_p(l_1) + \gamma_s^* I_p(l_1) - 2\gamma_p^s I_s(l_1) + \Delta)^2}{4}}, \end{aligned}$$

Here, $\psi = \psi_1 + \psi_2$, where $\psi_1 = 2\varphi_p(l_1) - \varphi_a(l_1) - \varphi_s(l_1) - \Delta l_1$ is the generalized phase of the waves during the passage of the first layer.

$$I_a(l_3) = I_a(l_2)\left[\left(\cos\lambda_3^a l_3 + c\frac{\sin\lambda_3^a l_3}{\lambda_3^a}\right)^2 + \left(b\frac{\sin\lambda_3^a l_3}{\lambda_3^a}\right)^2\right], \tag{13}$$

where

$$\begin{aligned} c &= \frac{\gamma_a^{sa\prime}}{\gamma_a^{sa}}\left[(\lambda_1^a \cot\lambda_1^a l_1 + \gamma_a I_{po})\cos\psi + \frac{\gamma_1^a - \Delta}{2}\sin\psi\right], \\ b &= \frac{\gamma_a^{sa\prime}}{\gamma_a^{sa}}\left[(\lambda_1^a \cot\lambda_1^a l_1 + \gamma_a I_{po})\sin\psi - \frac{\gamma_1^a - \Delta}{2}\cos\psi\right] - (\gamma_3 + \frac{\Delta'}{2}). \end{aligned}$$

It can be seen from expression (13) that the terms with l_1 enter $I_a(l_2)$ and into the expressions for the coefficients c and b (through $I_a(l_1)$. This leads to a change in the coherent length of the first layer for obtaining the maximum signal of the anti-Stokes component after three layers.

At $\lambda_1 l_{1,coh}^{CIA} = \pi/2$ the intensity $I_a(l_3)$ is equal to

$$I_a(l_3) = I_a(l_2)\times\left\{\left[\cos\lambda_3^a l_3 \pm \frac{\gamma_a^{sa\prime}}{\gamma_a^{sa}}\gamma_a I_{po}\frac{\sin\lambda_3^a l_3}{\lambda_3^a}\right]^2 + \left[\left(\pm\frac{\Delta - \gamma_1^a}{2}\cdot\left(\frac{\gamma_a^{sa\prime}}{\gamma_a^{sa}}\right) - \gamma_3 - \frac{\Delta'}{2}\right)\right]^2\left(\frac{\sin\lambda_3^a l_3}{\lambda_3^a}\right)^2\right\} \tag{14}$$

The upper sign corresponds to the case $\psi = 2\pi n$, and the lower sign corresponds to $\psi = (2n+1)\pi,\ n = \pm1,\ \pm2, \ldots$ Let us assume that the same nonlinear media are used in the first and third active layer, then for $\gamma_a^{sa} = \gamma_a^{sa\prime}$ we obtain:

$$I_a(l_3) = I_a(l_2)\left[\left(\cos\lambda_3^a l_3 \pm \gamma_a I_{po}\frac{\sin\lambda_3^a l_3}{\lambda_3^a}\right)^2 + \left(\pm\frac{\Delta - \gamma_1^a}{2} - \frac{\Delta'}{2} - \gamma_3\right)^2\left(\frac{\sin\lambda_3^a l_3}{\lambda_3^a}\right)^2\right]. \tag{15}$$

It follows from (15) that for an increase in the output intensity $I_a(l_3)$ at a constant phase mismatch ($\varDelta = \varDelta$) the case is favorable when the terms in brackets with the phase mismatch contribute of the same sign to $I_a(l_3)$ and thereby ensure its increase. This condition is observed at $\psi = \pi(2n+1)$. This conclusion also follows from Fig. 1 - 4 obtained by numerical calculation of the analytical expression (15) in CIA.

Note that the coherent lengths of the active layers and depend not only on the value of the phase mismatch, but also on the intensities of the pump wave and the Stokes component. Moreover, these parameters refer not only to the current third active layer ($\varDelta'$, $I_p(l_1)$, $I_s(l_1)$) , but also to the first active layer ($\varDelta, I_{po,so}$) .

3 Results and discussion

All graphical results obtained based on analytical formulas in the CIA are calculated for the parameters of a specific experiment [9-10] for compressed hydrogen. The article provides not just one numerical estimate of the conversion efficiency in the CIA for the parameters of a particular experiment using the obtained analytical formulas, but entire graphical dependences of the expected behavior of the conversion efficiency on various experimental parameters with specific recommendations for the optimal values of the problem parameters: coherent length, period of the phase matching curve etc. From (4), (5), (7), (8) and (15) obtained analytically in CIA, one can numerically analyze the behavior of the intensities and phases of the anti-Stokes and Stokes scattering components in a three-layer structure. In this case, we choose the parameters of the problem from existing experiments [9-10]. We choose the most active Raman medium as the active medium: compressed hydrogen (having a maximum combination shift at SRS among gases, equal to 4155 cm^{-1}). The second harmonic Nd:YAG (532 nm) was used as the pump wave. The wavelength of the Stokes (682.8 nm) and anti-Stokes components (435.69 nm) of SRS was determined from the frequency shift. These wavelengths are necessary when calculating the nonlinear coefficients of the scattering components. The pump intensity varied from tens of MW/cm^2 to tens of GW/cm^2. The phase mismatch Δ varied in the range of 2–15 cm^{-1} and the SRS gain for compressed H_2 varied in the range of 1–10 cm/GW.

The results of the numerical calculation of the corresponding expressions are presented in Figures 1–4. The curves are plotted for the case of identical phase mismatch values in each of the active layers ($\varDelta = \varDelta'$), optimal layer lengths, which are determined from the conditions $\lambda_{1,3}^{a} = \pi/2$ and in the absence of losses.

Figure 1 shows the dependences of the intensities of the scattering components in the first layer $I_a(l_1)$, using (4), and $I_s(l_1)$, using (5), for different values of the phase mismatch and input values of the intensity of the Stokes component I_{so} . In this case, the behavior of the dependence $I_a(l_1)$ with a phase mismatch is determined by the term $\frac{sinh\lambda_1^{a''} l_1}{\lambda_1^{a''}}$. which through the parameter $\lambda_1^{a''}$ depends on Δ (curves 3 and 4). Similarly, from (5) the behavior of the curves for the Stokes component is determined. The dependence $I_s(l_1)$ on the phase mismatch is contributed by term $\frac{\gamma_1^s - \varDelta}{2}$ the sine and cosine functions through the parameter λ_1^s . This explains the observed weak response $I_a(l_1)$ to the same change in the phase mismatch (curves 3 and 4) compared to $I_s(l_1)$ (curves 1 and 2). In addition, a change in the phase mismatch leads to a shift of the oscillations $I_s(l_1)$ along the longitudinal coordinate **Z** (curves 1 and 2). However, at different I_{so} (curves 3, 5, and 6), the period of oscillations practically does not change, which, as the analysis showed, relates to the smallness of the contribution of the term with I_{so}.

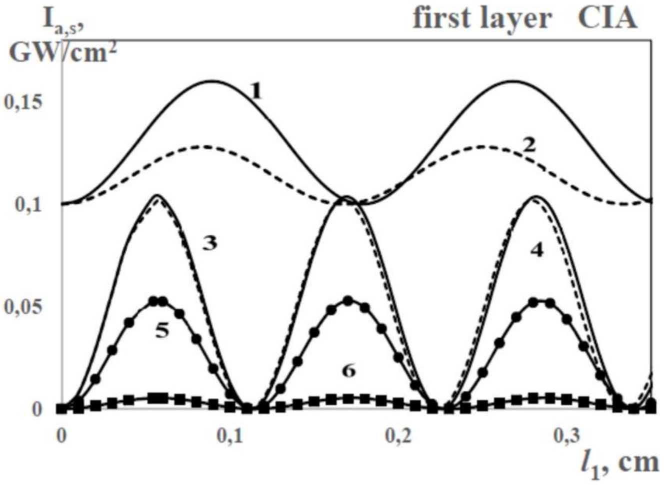

Figure 1. Dependences of the intensities of the scattering components in the first layer $I_a(l_1)$ (curves 3–6) and $I_s(l_1)$ (curves 1–2) for $I_{po} = 10$ GW/cm^2, $I_{ao} = 0$ at $\Delta = 13$ cm^{-1} (curves 2 and 4) and 15 cm^{-1} (curves 1, 3, 5, 6) and $I_{so} = 10^{-2} I_{po}$ (curves 1–4), $5 \cdot 10^{-3} I_{po}$ (curve 5), $5 \cdot 10^{-4} I_{po}$ (curve 6). We calculated the dependencies in CIA.

Figure 2, according to (7) and (8), shows the dynamics of the behavior of the phases of the pump wave and the anti-Stokes component as it moves along the z axis, calculated using (7) and (8). Intersection of lines indicates the optimal value of the length of the nonlinear medium (the coherent length), at which the maximum transfer of the energy of the exciting waves into the energy of the generated anti-Stokes wave occurs.

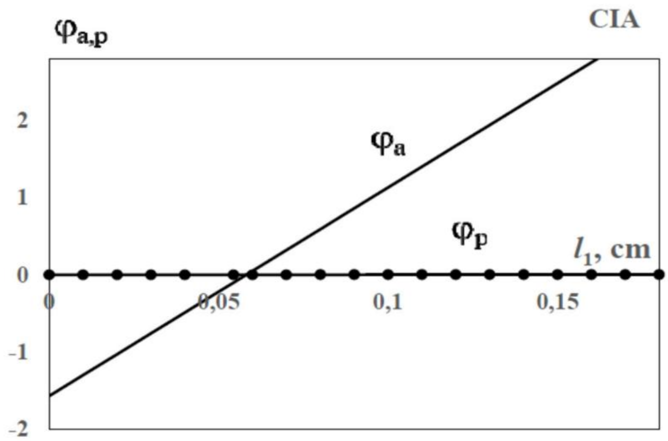

Figure 2. Dependences of the phases of the pump wave $\varphi_p(l_1)$ and the anti-Stokes component $\varphi_a(l_1)$ in the first layer for $I_{po} = 10$ GW/cm^2, $I_{ao} = 0$, $I_{so} = 10^{-2}I_{po}$, $\Delta = 3.84$ cm^{-1}. We calculated the dependences in CIA.

Figure 3 shows how, under conditions of quasi-phase matching, a gradual smooth increase in the intensity of the anti-Stokes component occurs in the first, using (4), and third, according to (15), active layers. In the second passive layer, the intensity does not change, a horizontal section is observed (see insert). As soon as the intensity maximum is reached in the first layer at the coherent length of the first layer $l_{1,\text{coh}}^{\text{CIA}} = 0.0544$ cm, the second passive layer starts. In the third layer, the maximum intensity is reached at the coherent length of the third layer $l_{3,\text{coh}}^{\text{CIA}} = 0.038$ cm. As can be seen from the comparison, the coherent lengths of the active layers decrease, which was also noted in [9-10]. This is the opposite of the result obtained in RDS [15]. This contradiction was explained by the authors of [6] with the non-multiplicity of the frequencies of the interacting waves. Note that the distance between the minima of the phase-matching curve in CIA, in contrast to CFA is not constant. This must be considered when calculating the phase matching width in similar layered structures.

From Fig. 3, it turns out that at coherent lengths of the first $l_{1,\text{coh}}^{\text{CIA}}$ and third active layers $l_{3,\text{coh}}^{\text{CIA}}$, the optimal phase relationship between the interacting waves and the optimal ratio I_{so}/I_{po} (see Figure 1) it is possible to increase the maximum conversion efficiency of the anti-Stokes component I_a/I_{po} from 0.01 in the first active layer to 0.026 in second active layer (see Figure 3). Comparison with Fig. 3 in [9] shows that a similar result realized there approximately on the 26th layer. By calculating the optimal parameters for each specific case, it is possible to increase the conversion efficiency even with a smaller number of active layers. The above calculations in CIA for two active media, if necessary, can be continued and applied to n number of layers, how we did it in the case of sum frequency generation in RDS.

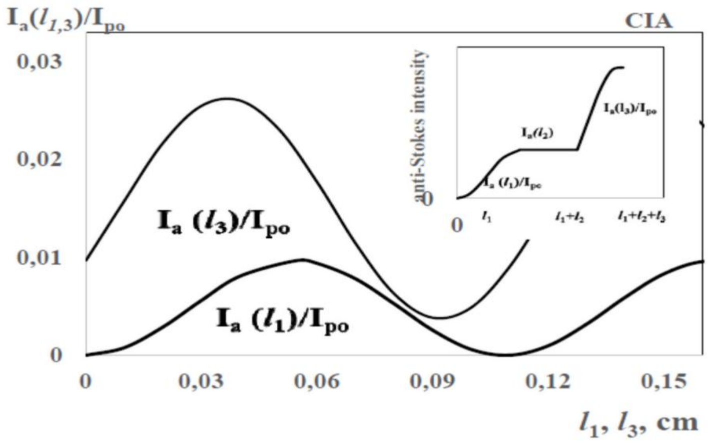

Figure 3. Dependences of the conversion efficiency of the anti-Stokes scattering component in the first $I_a(l_1)/I_{po}$ and third layers $I_a(l_3)/I_{po}$ for $I_{po} = 10$ GW/cm^2, $I_{ao} = 0$, $I_{so} = 10^{-2}I_{po}$ at $\Delta = 3.84$ cm^{-1}, $l_{1,\text{coh}}^{\text{CIA}} = 0.0544$ cm, $\psi = \pi(2n+1)$, $\psi_2 = \pi$. Insert: Dependency of $I_a(l_1, l_1+l_2, l_1+l_2+l_3)/I_{po}$. We calculated the dependencies in CIA.

Figure 4, according to (15), shows the dependence of the intensity of the anti-Stokes component in the third layer on the layer length $I_a(l_3)$ at different pump intensities. There is an optimal value I_{po} . For the given parameters of the problem $I_{po}^{\text{opt}} = 9$ GW/cm^2. With a change in the pump intensity, not only the intensity of the anti-Stokes component changes, but also the oscillation period, and we observed a shift of the minima. This is due to the $\lambda_{1,3}^a$ parameters associated with I_{po} . This does not take place in the CFA.

Thus, for a specific experiment, using the analytical expressions obtained in the CIA one can calculate the optimal values of the problem parameters to achieve the maximum conversion to the anti-Stokes component at quasi-phase matching interaction, and consider the case of dissipative media.

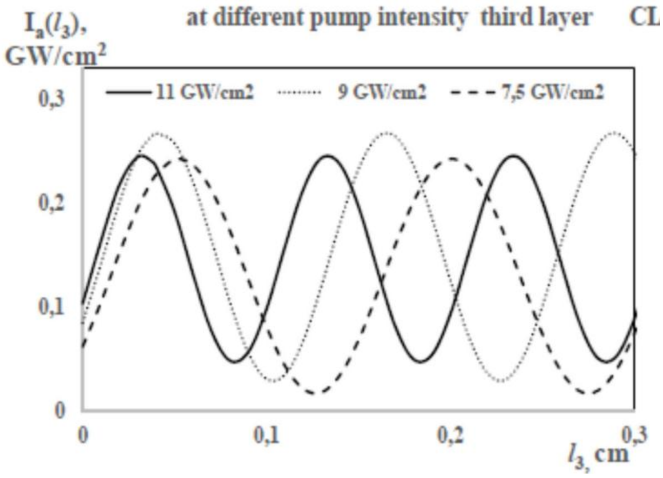

Figure 4. Dependence of the intensity of the anti-Stokes component in the third layer on the layer length $I_a(l_3)$ at $I_{po} = 7.5$ GW/cm^2 (dashed curve), 9 GW/cm^2 (dotted curve), and 11 GW/cm^2 (solid curve). We calculated the dependencies in CIA.

4 Conclusion

By calculating the optimal parameters of the problem (lengths of the active layers, phase detuning, pump and Stokes component intensities, optimal phase ratio), one can obtain high values of the conversion efficiency at the output of the layered structure even with a smaller number of active layers. Note that the coherent lengths of the active layers depend not only on the value of the phase mismatch, but also on the intensities of the pump wave and the Stokes component. Moreover, these parameters are not only for the current active layer, but also for the previous active layer. With a change in the pump intensity, not only the intensity of the anti-Stokes component changes, but also a period of oscillations, a shift of the minima occurs. Researchers need to consider this fact when calculating the phase matching width in layered structures. The dependence of the phase relations on the intensities of the interacting waves, considered in the CIA, is proof of a more correct study of the nonlinear interaction of optical waves in layered structures. There is no such dependence in the CFA.

REFERENCES

[1] V.G. Bespalov, A.M. Dukhovny, D.I. Staselko, "Investigation of the coherence of radiation during SRS in compressed hydrogen," Zh.TF Letters, 5(20), 1236-1239 (1979).

[2] R.B.Andreev, V.A. Gorbunov, S.S. Gulidov, S.B. Paperny, V.A. Serebryakov, "Rol of parametric effects in generation of higher components of stimulated Raman scattering in gases," Sov J Quantum Electron, 12(1), 35-37 (1982). DOI 10.1070/QE1982v012n01ABEH005260

[3] J.J. Ottusch, M.S. Mangir, D.A. Rockwell, "Efficient anti-Stokes Raman conversion by four-wave in gases," JOSA B, 8(1), 68-77 (1991). https://doi.org/10.1364/JOSAB.8.000068

[4] N. Blombergen. Nonlinear optics. W. A. Benjamin Inc. New York-Amsterdam, 424 (1965).

[5] M.M. Feje, G.A. Magel, D.H. Jund and R.L. Byer, "Qusi-phas-at c arma: and tolerances," IEEE J. Quantum Electronics, 28(11), 2631-2654 (1992). DOI: 10.1109/3.161322

[6] Rian Stuart Coetzee, Andrius Zukauskas, Carlota Canalias, Valdas Pasiskevicius. "Low-threshold, mid-infrared backward-wave parametric oscllator with periodically poled Rb:KTP," APL Photonics 3, 071302 (2018), https://doi.org/10.1063/1.5035493.

[7] Anne-Lise Viotti, Fredrik Laurell, Andrius Zukauskas, Carlota Canalias, and Valdas Pasiskevicius, "Coherent phase transfer and pulse compression at 1.4μm in a backward-wave OPO," Opt. Lett. 44, 3066-3069 (2019), https://doi.org/10.1364/OL.44.003066.

[8] VoL Zukuskas, Canalias, Laure, Pasiskevicus. "Narrwband tuable, ifraradian y parametric amplification of a chirped backward-wave OPO signal," Opt Express. 27(8), 10602-10610 (2019), doi: 10.1364/OE.27.010602. PMID: 31052916.

[9] V.G Bespalov, N.S. Makarov, "Quasi-phase matching generation ofblue coherent radiation at stimulatedRaman scattering," Optics Communications, 203, Issues 3-6, 413-420 (2002). https://doi.org/10.1016/S0030-4018(02)01166-5

[10] V.G. Bespalov, N.S. Makarov, "SRS generation of anti-Stokes radiation under phase quasi-matching conditions," Optics and spectroscopy, 90(6), 1035-1038 (2001). https://doi.org/10.1134/1.1380796

[11] YuA. Iyisky. DTn, "On hetial Starec aRamttin a," Q Electronics, 1(7), 1500-1506 (1974).

[12] A.S. Chirkin, V.V. Volkov, G.D. Laptev, E.Yu. Morozov, “Consecutive three-wave interactions in nonlinear optics of periodically inhomogeneous media,” Quantum Electronics, 30(10) 847-858 (2000). DOI: https://doi.org/10.1070/QE2000v030n10ABEH001859

[13] M.M. Fejer, in: Beam Shaping and Control with Nonlinear Optics, Plenum Press, New-York, 1998, p. 375.

[14] R.L. Byer, “Quasi-phase matched nonlinear interactions and devices,” Nonlinear Opt. Phys. Materials, 6, 549-553 (1997).

[15] J.D. McMullen, “Optical parametric interactions in isotropic materials using a phase-corrected stack of nonlinear dielectric plates,” J. Appl. Phys., 46, 3076-3081 (1975). https://doi.org/10.1063/1.322001

[16] K.C. Rustagi, S.C. Mehendale, and S. Meenakshi, “Optical frequency conversion in quasi-phase-matched stacks of nonlinear crystals,” IEEE J. Quantum Electronics, 18(6), 1029-1041 (1982). DOI: 10.1109/JQE.1982.1071650

[17] Z.H. Tagiev, A. Chirkin, “Fixed-intensity approximation in the theory of nonlinear waves,” Zh. Exp T. Fiz. 73, 1271-1282 (1977); Z.H. Tagiev, R.J. Kasumova, R.A. Salmanova, N.V. Kerimova, “Constant intensity approximation in a nonlinear wave theory,” J. Opt. B: Quantum Semiclas. Opt., 3, 84 (2001). DOI: https://iopscience.iop.org/article/10.1088/1464-4266/3/3/302/pdf

[18] Z.H. Tagiev, R.J. Kasumova, R.A. Salmanova, “Constant intensity approximation in sum frequency generation,” Opt. Commun., 281, 814-823 (2008). DOI:10.1016/j.optcom.2007.10.083

[19] Rena J. Kasumova, “Raman scattering at the intracavity parametric interaction,” Appl. Optics, 40(30), 5517 (2001). DOI: https://doi.org/10.1364/AO.40.005517

[20] R.J. Kasumova, N.V. Kerimova, G.A. Safarova, “Phase effects on coherent anti-Stokes Raman scattering,” J. Appl. Spectroscopy, 88(1), 17-24 (2021). https://doi.org/10.1007/s10812-021-01134-2

[21] Y.R. Shen, Principles of Nonlinear Optics, Wiley, New York, 1984.

[22] N. Vermeulen, C. Debaes, H. Thienpont, IEEE Journal of Quantum Electronics, 44(12), 1248-1255 (2009).

[23] Z.H. Tagiev, Rena J. Kasumova, “Theoretical studies on frequency doubling in glass optical fibers in constant intensity approximation,” Optics & Communications, 261, 258-265 (2006). https://doi.org/10.1016/j.optcom.2005.12.010